






## Article

# Availability of Central $\alpha 4\beta 2^*$ Nicotinic Acetylcholine Receptors in Human Obesity

Eva Schweickert de Palma <sup>1,2,\*</sup> , Tilman Günnewig <sup>1,2</sup>, Michael Rullmann <sup>1,2,3</sup> , Julia Luthardt <sup>1</sup>, Mohammed K. Hankir <sup>4</sup>, Philipp M. Meyer <sup>1</sup>, Georg-Alexander Becker <sup>1</sup>, Marianne Patt <sup>1</sup>, Sarah Martin <sup>2</sup>, Anja Hilbert <sup>5</sup> , Matthias Blüher <sup>6,7,8</sup> , Osama Sabri <sup>1,†</sup> and Swen Hesse <sup>1,2,†</sup> 

- <sup>1</sup> Department of Nuclear Medicine, University of Leipzig, 04013 Leipzig, Germany  
<sup>2</sup> Integrated Research and Treatment Center Adiposity Diseases, Leipzig University Medical Centre, 04103 Leipzig, Germany  
<sup>3</sup> Max Planck Institute for Human Cognitive and Brain Sciences, 04103 Leipzig, Germany  
<sup>4</sup> Department of General, Visceral, Transplantation, Vascular and Pediatric Surgery, University Hospital Wuerzburg, 97080 Wuerzburg, Germany  
<sup>5</sup> Department of Psychosomatic Medicine and Psychotherapy, Integrated Research and Treatment Center Adiposity Diseases, Behavioral Medicine Research Unit, University of Leipzig Medical Center, 04103 Leipzig, Germany  
<sup>6</sup> Helmholtz Institute for Metabolic, Obesity and Vascular Research (HI-MAG), Helmholtz Zentrum München at the University of Leipzig and University Hospital Leipzig, 04103 Leipzig, Germany  
<sup>7</sup> Medical Department III-Endocrinology, Nephrology, Rheumatology, University of Leipzig Medical Center, 04013 Leipzig, Germany  
<sup>8</sup> Collaborative Research Centre 1052 Obesity Mechanisms, University of Leipzig, 04103 Leipzig, Germany  
\* Correspondence: eva.schweickert@gmx.net  
† These authors contributed equally to this work.



**Citation:** Schweickert de Palma, E.; Günnewig, T.; Rullmann, M.; Luthardt, J.; Hankir, M.K.; Meyer, P.M.; Becker, G.-A.; Patt, M.; Martin, S.; Hilbert, A.; et al. Availability of Central  $\alpha 4\beta 2^*$  Nicotinic Acetylcholine Receptors in Human Obesity. *Brain Sci.* **2022**, *12*, 1648. <https://doi.org/10.3390/brainsci12121648>

Academic Editor: Ike C. de La Peña

Received: 25 October 2022

Accepted: 24 November 2022

Published: 1 December 2022

**Publisher's Note:** MDPI stays neutral with regard to jurisdictional claims in published maps and institutional affiliations.



**Copyright:** © 2022 by the authors. Licensee MDPI, Basel, Switzerland. This article is an open access article distributed under the terms and conditions of the Creative Commons Attribution (CC BY) license (<https://creativecommons.org/licenses/by/4.0/>).

**Abstract:** Purpose: Obesity is thought to arise, in part, from deficits in the inhibitory control over appetitive behavior. Such motivational processes are regulated by neuromodulators, specifically acetylcholine (ACh), via  $\alpha 4\beta 2^*$  nicotinic ACh receptors (nAChR). These nAChR are highly enriched in the thalamus and contribute to the thalamic gating of cortico-striatal signaling, but also act on the mesoaccumbal reward system. The changes in  $\alpha 4\beta 2^*$  nAChR availability, however, have not been demonstrated in human obesity thus far. The aim of our study was, thus, to investigate whether there is altered brain  $\alpha 4\beta 2^*$  nAChR availability in individuals with obesity compared to normal-weight healthy controls. Methods: We studied 15 non-smoking individuals with obesity (body mass index, BMI:  $37.8 \pm 3.1$  kg/m<sup>2</sup>; age:  $39 \pm 14$  years, 9 females) and 16 normal-weight controls (non-smokers, BMI:  $21.9 \pm 1.7$  kg/m<sup>2</sup>; age:  $28 \pm 7$  years, 13 females) by using PET and the  $\alpha 4\beta 2^*$  nAChR selective (–)-[<sup>18</sup>F]flubatine, which was applied within a bolus-infusion protocol ( $294 \pm 16$  MBq). Volume-of-interest (VOI) analysis was performed in order to calculate the regional total distribution volume (V<sub>T</sub>). Results: No overall significant difference in V<sub>T</sub> between the individuals with obesity and the normal-weight volunteers was found, while the V<sub>T</sub> in the nucleus basalis of Meynert tended to be lower in the individuals with obesity ( $10.1 \pm 2.1$  versus  $11.9 \pm 2.2$ ;  $p = 0.10$ ), and the V<sub>T</sub> in the thalamus showed a tendency towards higher values in the individuals with obesity ( $26.5 \pm 2.5$  versus  $25.9 \pm 4.2$ ;  $p = 0.09$ ). Conclusion: While these first data do not show greater brain  $\alpha 4\beta 2^*$  nAChR availability in human obesity overall, the findings of potentially aberrant  $\alpha 4\beta 2^*$  nAChR availability in the key brain regions that regulate feeding behavior merit further exploration.

**Keywords:** obesity; PET; acetylcholine; nicotinic receptors; (–)-[<sup>18</sup>F]flubatine; nucleus basalis of Meynert; thalamus

## 1. Introduction

Obesity is a major public health challenge worldwide. Understanding the processes that contribute to this pandemic is of significant clinical importance as obesity is strongly

associated with an increased risk of all-cause morbidity and mortality [1]. The complex physiological process of food intake is necessary for survival and is governed by the homeostatic system and the hedonic systems in the human brain [2]. An imbalance of these two systems can lead to weight gain and obesity [3].

The homeostatic system is located in the hypothalamus, while the hedonic system comprises cortico-limbic-striatal circuits. The main goal of the hypothalamic circuits is to balance the energy intake with the energy expenditure, specifically to balance the food intake with the metabolic needs, whereas the cortico-limbic-striatal circuits cover the affective and pleasurable components of food reward [2,3].

Neurotransmitters, such as dopamine (DA) and serotonin, are crucial for regulating food reward [4]. Brain imaging studies currently suggest lower striatal D2/D3 receptor binding potential in extreme obesity and a higher binding potential in overweight individuals and those with moderate obesity [5], depicting an important but complex role of DA in human obesity.

A neurotransmitter that is known to modulate DA release in the reward system (e.g., the nucleus accumbens (Nac) and the ventral tegmental area (VTA)) is acetylcholine (ACh) [6]. Nicotinic ACh receptors (nAChR) are highly expressed on the dopamine terminals, in the reward circuits, and in the areas of inhibitory control [3]. The thalamus has the highest density of certain subtypes of nAChR [7–9]. Nicotine, as an exogenous agonist on AChR, has a strong influence on the appetite, weight control, and food reward. Smokers are known to gain weight when they are quitting [10], while high-restrained eating is associated with elevated rates of smoking compared to the general population [11], and nicotine suppresses the appetite even in healthy non-smoking individuals [12]. Moreover, nicotinic agonists decrease food intake, body mass index (BMI, kg/m<sup>2</sup>), and weight gain by activating the hypothalamic pro-opiomelanocortin (POMC) neuron pathway through the central activation of  $\alpha 3\beta 4^*$  nAChR [13,14].

One of the major subtypes of nAChR that is expressed in the brain, the  $\alpha 4\beta 2^*$  nAChR, has been frequently associated with the mesoaccumbal reward system [3]. Studies have shown that these high-affinity  $\alpha 4\beta 2^*$  nAChR have an effect on the brain circuitries that are involved in reinforcement, mood, attention, and food consumption [15] through modulating DA release in the Nac [6,7]. In addition, the peripheral  $\alpha 4\beta 2^*$  nAChR are known to mediate the effect of nicotine, potentiating satiation and delaying food transit through a vago-vagal reflex [16]. A key role of  $\alpha 4\beta 2^*$  nAChR in both food reward and appetite control, and hence weight gain and the development of obesity, can therefore be assumed.

However, despite this apparently important role in energy balance, *in vivo* imaging on  $\alpha 4\beta 2^*$  nAChR by using positron emission tomography (PET) and radiotracers that are selective for  $\alpha 4\beta 2^*$  nAChR, such as (–)-[<sup>18</sup>F]flubatine [9] in humans, have not been performed to date. In order to depict the alterations of modulatory  $\alpha 4\beta 2^*$  nAChR availability in the brain regions that are relevant for eating control, an investigation of  $\alpha 4\beta 2^*$  nAChR availability in these brain regions could be a step forward in finding healthy alternatives to smoking for weight control [17].

In this exploratory study, we therefore investigated for the first time *in vivo*  $\alpha 4\beta 2^*$  nAChR availability in individuals with obesity compared with normal-weight volunteers using PET and the radiotracer (–)-[<sup>18</sup>F]flubatine [9,18]. The regions of interest include the brain areas that are important in eating circuits (Nac, VTA, the orbitofrontal cortex (OFC), the prefrontal cortex (PFC), the amygdala, and the insula), as well as the core regions of the central cholinergic system (nucleus basalis of Meynert (NBM) and the thalamus). We hypothesized that, in these core areas of the basal forebrain and the thalamo-cortical system specifically, the  $\alpha 4\beta 2^*$  nAChR availability is altered in the individuals with obesity compared to the normal-weight healthy controls.

## 2. Materials and Methods

This clinical study was performed according to the 1964 declaration of Helsinki and subsequent revisions and was approved by the local ethics committee (number 225-15-01062015), as well as the national radiation protection agency. The trial is registered at the Deutsches Register für klinische Studien (DRKS) under DRKS00010927.

### 2.1. Study Participants

We consecutively included 15 volunteers with obesity with a BMI of  $>35 \text{ kg/m}^2$  and 16 normal-weight volunteers with a BMI of  $<25 \text{ kg/m}^2$ . All of the study participants were non-smokers, were free for any kind of centrally acting medication, and had no history of neurological or psychiatric illness. They were recruited from public postings and nutritional therapy groups. The exclusion criteria were as follows: neurosurgery in the past, structural tissue lesions, the use of medication or surgery for weight reduction in the last six months, a vegan diet, and contraindications for magnetic resonance imaging (MRI). All of the study participants were asked to complete the Three-Factor Eating Questionnaire (TFEQ, [19]), which measures three dimensions of eating behavior ('disinhibition', 'hunger', and 'cognitive restraint'). The normal-weight volunteers with a score that was higher than seven points in the subscale 'disinhibition' of the TFEQ were excluded.

### 2.2. PET/MRI Acquisition Protocol and Processing

The  $(-)-[^{18}\text{F}]\text{flubatine}$  was synthesized according to a fully automated and GMP-compliant procedure utilizing a commercially available synthesis module (TRACERlab FX FN) [20]. To avoid arterial blood sampling, PET was performed by applying a bolus plus constant infusion (B/I) protocol, according to Hillmer et al. [18], using the PET/MRI Biograph mMR system (Siemens) as follows: after a 90 s intravenous bolus of  $202 \pm 6 \text{ MBq}$   $(-)-[^{18}\text{F}]\text{flubatine}$ ,  $91 \pm 15 \text{ MBq}$  (98 mL solution with an hourly rate of 0.6 mL/min) was constantly infused to the end of an in-total scanning time of 165 min, resulting in a total administered activity of  $294 \pm 16 \text{ MBq}$   $(-)-[^{18}\text{F}]\text{flubatine}$  (Table 1). Starting with the bolus injection (minute zero), the dynamic PET data were acquired in list-mode through a standardized high resolution 3D imaging protocol sequentially to 60 post injection (p.i.; 20 frames with  $4 \times 15 \text{ s}$ ,  $4 \times 60 \text{ s}$ ,  $5 \times 120 \text{ s}$ ,  $5 \times 300 \text{ s}$ , and  $2 \times 600 \text{ s}$ ) and between 120 and 165 p.i. (13 frames with  $12 \times 212 \text{ s}$  and  $1 \times 156 \text{ s}$ ).

**Table 1.** Demographics and Three-Factor Eating Questionnaire scores of individuals with obesity and normal-weight controls.

Variables	Individuals with Obesity (n = 15)	Normal-Weight Controls (n = 16)	p Value
Age (years)	$39.5 \pm 14.0$ (20 to 62)	$27.5 \pm 7.3$ (19–45)	0.005 <sup>a</sup>
Sex (male/female)	6/9	3/13	0.25 <sup>b</sup>
BMI ( $\text{kg/m}^2$ )	$37.8 \pm 3.1$ (32.5 to 42.8)	$21.9 \pm 1.7$ (19.4 to 24.9)	$<0.001$ <sup>a</sup>
Activity (MBq)	$291 \pm 8.5$ (270 to 300)	$295 \pm 8.0$ (273 to 307)	0.15 <sup>a</sup>
TFEQ score			
Cognitive control	$8.7 \pm 5.5$ (1 to 19)	$7.2 \pm 3.9$ (2 to 15)	0.37 <sup>a</sup>
Disinhibition	$8.9 \pm 3.6$ (3 to 14)	$3.4 \pm 2.1$ (0 to 7)	$<0.001$ <sup>a</sup>
Hunger	$5.6 \pm 2.6$ (2 to 9)	$3.2 \pm 2.8$ (0 to 10)	0.02 <sup>a</sup>

Mean  $\pm$  SD (range); <sup>a</sup> Student's *t*-test; <sup>b</sup> exact Fisher test; SD: standard deviation; BMI: body mass index; TFEQ: Three-Factor Eating Questionnaire.

The PET data were corrected for attenuation using ultra-short echo time sequences (UTE) [21], scatter, and radioactive decay and were reconstructed into  $256 \times 256 \times 127$  matrix with  $1.0 \times 1.0 \times 2.03 \text{ mm}^3$  voxel size using the built-in 3D ordered subset expectation maximization algorithm with 8 iterations, 21 subsets, and a 3 mm Gaussian filter. The MRI sequences included a high-resolution T1-weighted 3D magnetization-prepared rapid gradient-echo (MPRAGE) (repetition time: 1900 ms, echo time: 2.53 ms, inversion time: 900 ms) sequence to perform anatomical mapping for the generation of volumes of interest

(VOIs) in the PET data sets. UTE sequences were acquired shortly before the radiotracer bolus administration, while the MPRAGE was obtained within the first minutes thereafter.

The PET and MRI data were processed further using PMOD (version 3.5, PMOD Technologies, Zurich, Switzerland). First, eight VOIs were drawn manually on consecutive transversal slices of the individual MRI data sets in the brain areas that are relevant for feeding control and the core regions of the brain cholinergic system (amygdala, insula, NAc, NBM, OFC, PFC, thalamus, and VTA; Figure 1). Then, the PET data were corrected for head motion artifacts and were co-registered with the individual MRI data and the related VOI set to obtain corresponding tissue time activity curves (TACs) from the dynamic PET data (Figure 2).

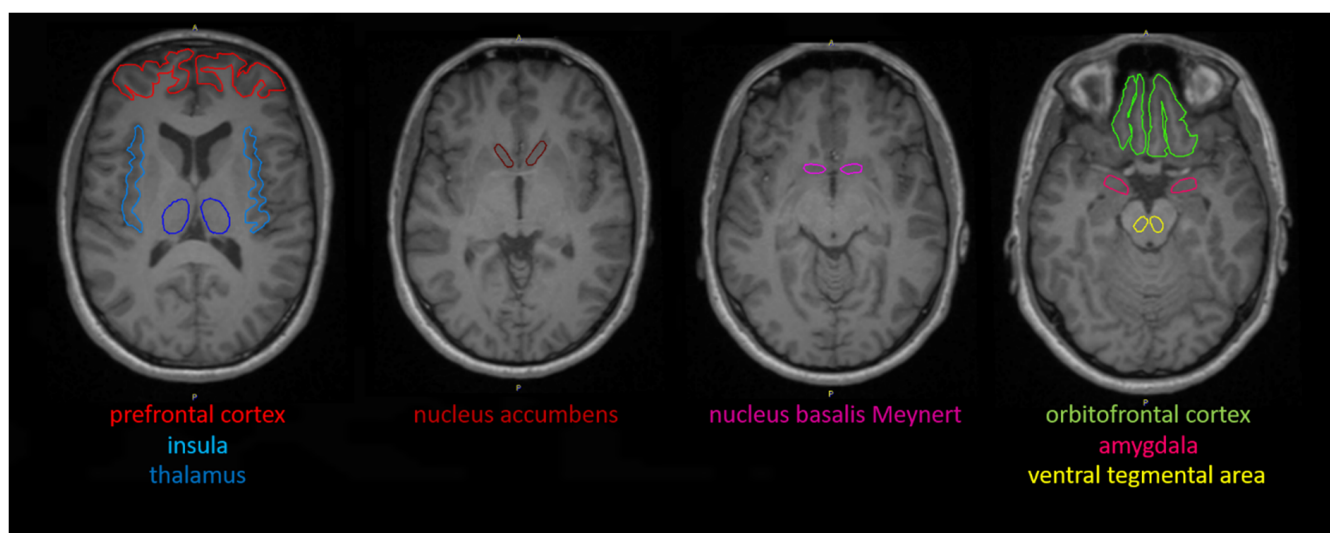


**Figure 1.** Manually drawn, anatomical-based volumes of interest defined in individual transaxial magnetic resonance imaging data sets (same text color was used for the specific brain region in each slice).

For the calculation of the total distribution volume ( $V_T$ ), venous blood samples at 90 min, 105 min, 120 min, 135 min, 150 min, and 160 min p.i. with four probes of 2 mL at each time point, resulting in a total blood volume of 48 mL ( $6 \times 4 \times 2$  mL), were taken. The 120–165 min p.i. tracer concentration in tissue ( $C_{\text{tissue}}$ ) at equilibrium were divided by the total radioactivity concentration in the venous plasma ( $C_{\text{plasma}}$ ) to generate the total distribution volume ( $V_T$ ) for each VOI. For an optimal bias-variance tradeoff, metabolite correction was not considered in the present analysis. This is because our own previous pilot data using the arterial input function without metabolite correction yielded only slightly (about 10%) lower distribution volumes for all regions, since the uncorrected input function at 90 min is about 10% higher. Nevertheless, the relative standard deviation of  $V_T$  was lower with the input functions without metabolite correction [9].

### 2.3. Statistical Analyses

The statistical analyses were performed with Jamovi 1.6.23. A Student's *t*-test and exact Fisher test (significance at  $p < 0.05$ ; Table 1) were performed to test for group differences. As 'age' differed between the normal-weight volunteers and the individuals with obesity, we used ANCOVA with age as a covariate to compare the  $V_T$  of both study groups. The correlation of  $V_T$  with subscales of TFEQ separately for participants with obesity and normal-weight participants were analyzed through partial correlation controlling for age.

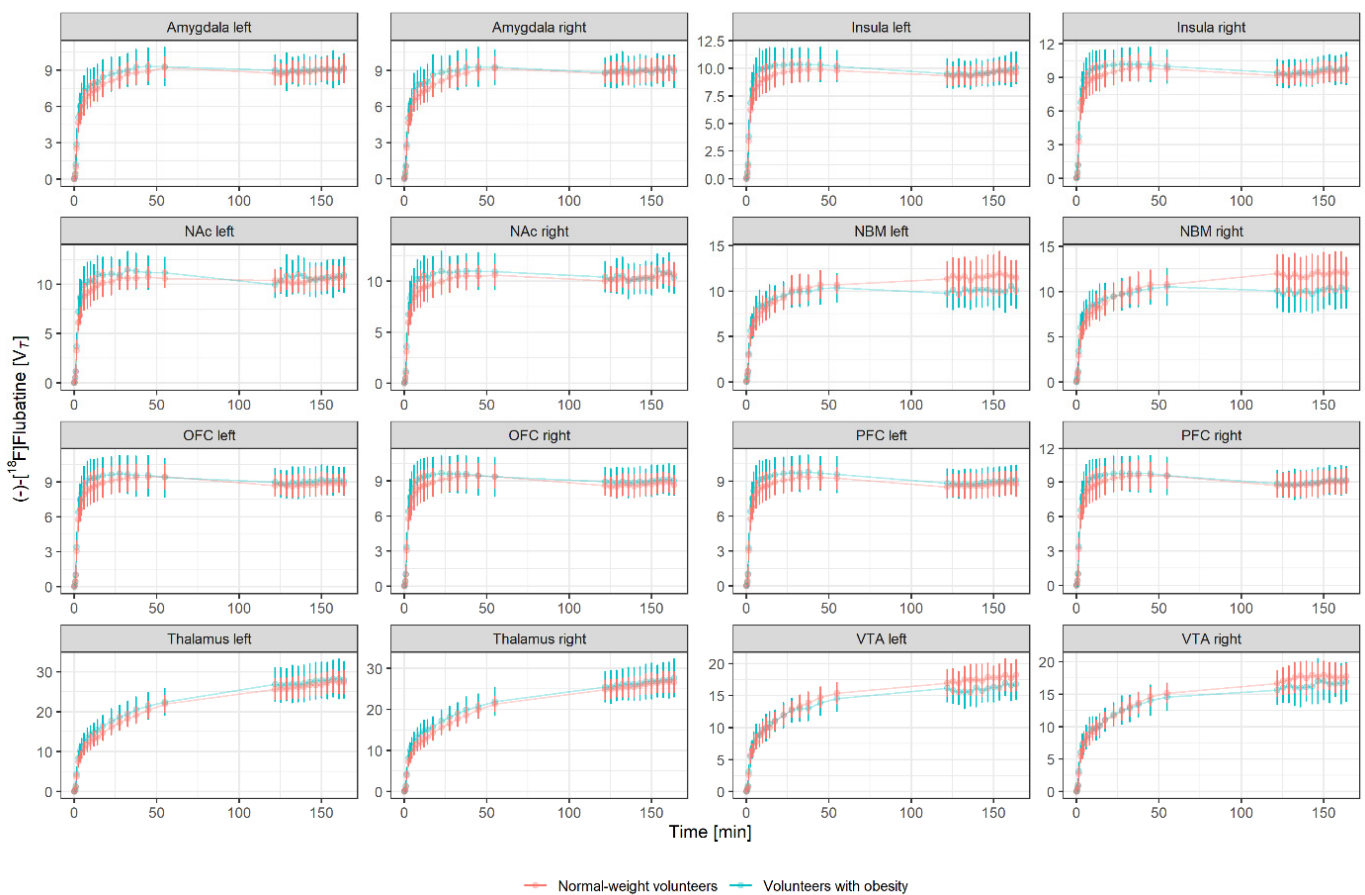


**Figure 2.** Generated average time activity curves after applying (–)-[<sup>18</sup>F]flubatine in a bolus plus constant infusion protocol of both study cohorts for each volume of interest; first phase from 0 to 60 min p.i. consisting of 20 frames and second phase from 120 to 165 min p.i. consisting of 13 frames.

### 3. Results

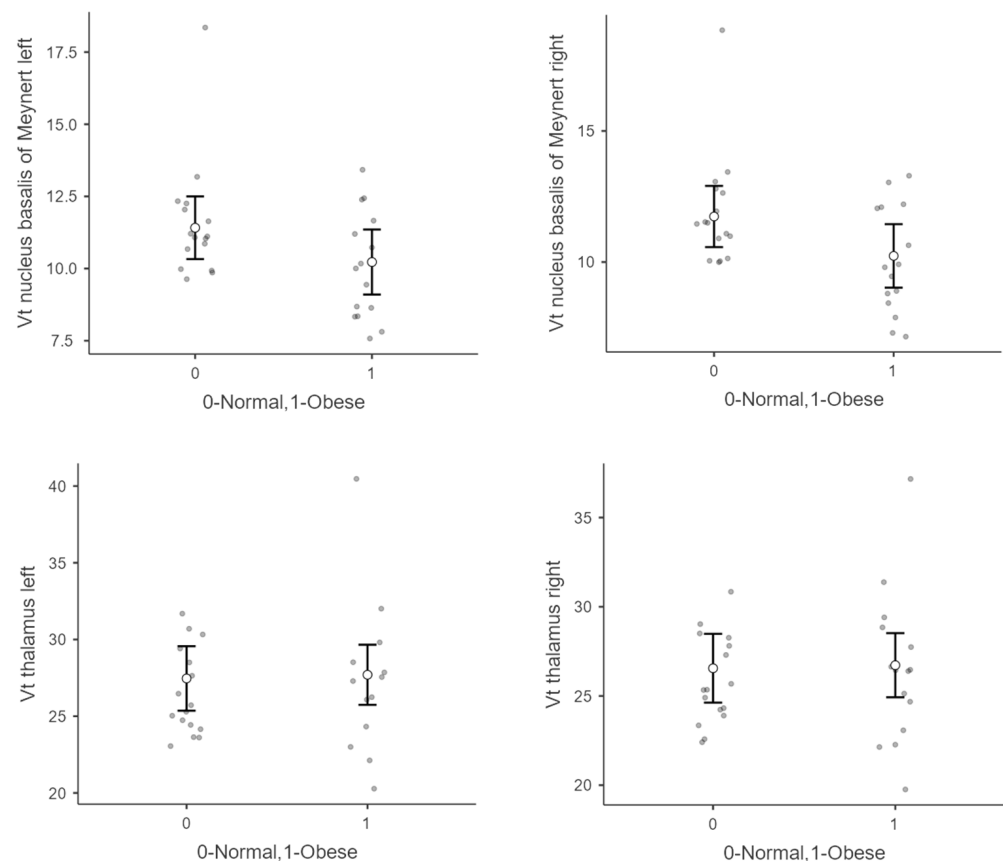
Table 1 shows the demographic data of the study participants. The age was significantly higher in the individuals with obesity compared with the normal-weight volunteers, while the TFEQ scores of ‘disinhibition’ and ‘hunger’ were significantly lower in the normal-weight controls compared to the individuals with obesity.

Table 2 presents the  $V_T$  in the individuals with obesity and the normal-weight volunteers, controlled for age. Overall, no significant differences in  $V_T$  between the individuals with obesity and the normal-weight controls were found. The  $V_T$  in the NBM tended to be lower in the volunteers with obesity compared with the normal-weight volunteers (Table 2, Figure 3), while the  $V_T$  in the thalamus showed a tendency towards higher values in the volunteers with obesity versus the normal-weight volunteers (Table 2, Figure 3). The mean  $V_T$  of the normal-weight volunteers and the volunteers with obesity is shown in Figure 4.

A correlation heatmap of all of the VOIs is shown in Figure 5. The  $V_T$  of the NBM appears to be less associated with the  $V_T$  of all of the other regions, particularly in the normal-weight controls, while the interregional correlations seem to be stronger in the volunteers with obesity versus the normal-weight volunteers.

**Table 2.** Comparison of total distribution volumes ( $V_T$ ) in regions of interest between individuals with obesity and normal-weight controls.

Region		Individuals with Obesity ( $n = 15$ )		Normal-Weight Controls ( $n = 16$ )		$p^a$
		Mean	SD	Mean	SD	
Amygdala	Left	9.00	1.2	8.91	0.9	0.55
	Right	8.99	1.3	8.93	0.9	0.66
Insula	Left	9.63	1.3	9.49	0.9	0.40
	Right	9.55	1.3	9.40	0.9	0.44
Nucleus accumbens	Left	10.60	1.7	10.40	1.0	0.62
	Right	10.40	1.5	10.40	1.0	0.70
Nucleus basalis of Meynert	Left	10.10	1.9	11.60	2.1	0.16
	Right	10.10	2.1	11.90	2.2	0.10
Orbitofrontal cortex	Left	9.03	1.3	8.77	0.9	0.46
	Right	8.97	1.3	8.68	0.9	0.42
Prefrontal cortex	Left	8.88	1.3	8.67	1.1	0.35
	Right	8.96	1.2	8.87	1.1	0.43
Thalamus	Left	27.40	4.7	26.50	2.8	0.15
	Right	26.50	4.2	25.90	2.5	0.09
Ventral tegmental area	Left	16.10	2.2	17.60	2.2	0.38
	Right	16.40	2.6	17.50	2.1	0.61

<sup>a</sup> ANCOVA with age as covariate.**Figure 3.** Total distribution volume ( $V_T$ ) of (-)-[<sup>18</sup>F]flubatine in individuals with obesity and normal-weight controls in the right and left nucleus basalis of Meynert and the right and left thalamus shown as jitter plots. The mean value is depicted with the white point and error bars representing the standard deviation. Individual data points are represented in gray.

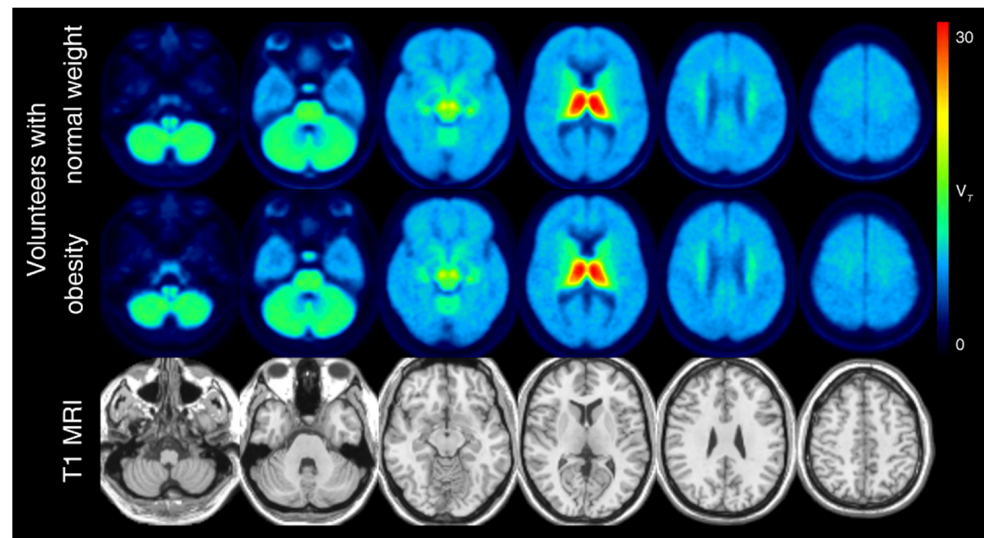


**Figure 4.** The  $(-)$ - $[^{18}\text{F}]$ flubatine average total distribution volume of all normal-weight volunteers (first row) and volunteers with obesity (second row) using positron emission tomography co-registered to T1 (third row) magnetic resonance imaging.

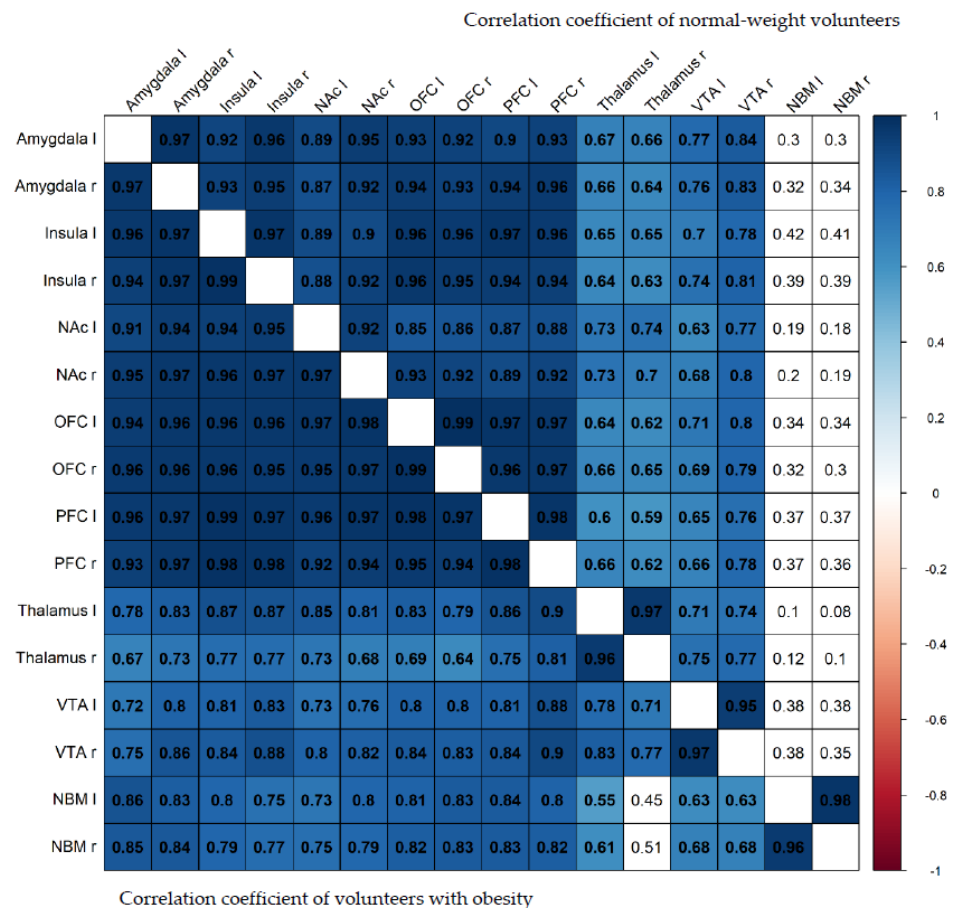


**Figure 5.** Correlation heatmap showing the strength of correlations between all volumes of interest, while blue indicates a positive correlation and red a negative correlation ( $p < 0.05$ ). Fields with a white background represent non-significant correlations ( $p > 0.05$ ). A partial correlation of  $V_T$  with subscales of the TFEQ performed separately for individuals with obesity and normal-weight controls showed that none of the TFEQ subscales correlated significantly with  $V_T$  (Table 3).

**Table 3.** Partial correlation of total distribution volume ( $V_T$ ) with subscales of the Three-Factor Eating Questionnaire (cognitive control, disinhibition, and hunger) in individuals with obesity ( $n = 15$ ) and in normal-weight controls ( $n = 16$ ).

Region			Individuals with Obesity ( $n = 15$ )			Normal-Weight Controls ( $n = 16$ )		
			Control	Disinhibition	Hunger	Control	Disinhibition	Hunger
Amygdala	Left	r	−0.125	−0.114	0.251	0.127	0.327	0.137
		p	0.460	0.698	0.387	0.653	0.235	0.628
	Right	r	−0.261	0.007	0.333	0.186	0.292	0.191
		p	0.367	0.982	0.245	0.506	0.292	0.495
Insula	Left	r	−0.241	0.087	0.432	0.124	0.194	0.160
		p	0.406	0.767	0.123	0.660	0.488	0.569
	Right	r	−0.254	−0.005	0.403	0.150	0.289	0.200
		p	0.381	0.987	0.153	0.594	0.297	0.475
Nucleus accumbens	Left	r	−0.375	−0.015	0.320	−0.011	0.278	0.153
		p	0.186	0.959	0.265	0.970	0.315	0.587
	Right	r	−0.319	0.077	0.382	0.183	0.483	0.362
		p	0.266	0.793	0.178	0.514	0.068	0.185
Nucleus basalis of Meynert	Left	r	−0.274	0.047	0.219	−0.150	0.276	0.117
		p	0.344	0.873	0.452	0.595	0.320	0.679
	Right	r	−0.257	0.080	0.275	−0.047	0.119	0.067
		p	0.374	0.785	0.342	0.868	0.673	0.811
Orbitofrontal cortex	Left	r	−0.318	−0.045	0.380	0.320	0.321	0.245
		p	0.268	0.879	0.180	0.244	0.243	0.379
	Right	r	−0.307	−0.065	0.408	0.310	0.310	0.272
		p	0.286	0.825	0.148	0.260	0.260	0.326
Prefrontal cortex	Left	r	−0.347	0.142	0.467	0.225	0.263	0.205
		p	0.225	0.628	0.092	0.350	0.344	0.464
	Right	r	−0.279	0.068	0.449	0.223	0.374	0.170
		p	0.334	0.819	0.108	0.424	0.170	0.545
Thalamus	Left	r	−0.491	−0.193	0.144	0.306	0.043	0.079
		p	0.334	0.509	0.623	0.267	0.89	0.781
	Right	r	−0.356	0.007	0.153	0.236	0.020	0.048
		p	0.211	0.980	0.602	0.396	0.944	0.865
Ventral tegmental area	Left	r	−0.291	0.061	0.523	0.210	0.038	0.183
		p	0.313	0.836	0.055	0.452	0.892	0.515
	Right	r	−0.300	0.015	0.449	0.257	0.118	0.285
		p	0.298	0.960	0.107	0.356	0.675	0.302

Spearman's rho Note: controlling for age.

#### 4. Discussion

This study investigated for the first time in vivo  $\alpha 4\beta 2^*$  nAChR availability in the brain regions that are important in feeding circuits in volunteers with obesity compared to normal-weight volunteers. Overall, no significant differences in  $\alpha 4\beta 2^*$  nAChR availability were found between the study groups. However, a tendency for lower  $V_T$  in the NBM in the volunteers with obesity, as well as a tendency for higher  $V_T$  in the thalamus, was found.

Besides the hypothalamus and the brainstem, the thalamus serves as an important independent input region for cholinergic signaling and functions [22]. Through cholinergic neuromodulation, the thalamus responds to external cues [23] and has the highest density of  $\alpha 4\beta 2^*$  nAChRs [7–9]. It is one of the most important brain regions modulating attentional control [24,25]. An example of this is given in the computational modeling of Schmitt et al. [25] as follows: enhanced mediodorsal thalamic (MD) excitability increased the PFC rule information content by improving the tuning of individual cortical neurons and also by recruiting the previously untuned cortical neurons. A thalamic circuit such as the MD therefore amplifies the local cortical connectivity in order to sustain the attentional control. A higher receptor availability in the volunteers with obesity than in the normal-weight volunteers in this region could hint to a higher receptiveness towards incoming cues, in this case food stimuli. Regarding the receptor dynamics, preliminary data applying



stimulation indicated that the  $\alpha 4\beta 2^*$  nAChR availability underlies the changes in the response to high-salient food cues [26]. Further and more extensive investigations, including studies that explore  $\alpha 4\beta 2^*$  nAChR availability with stimulation designs and functional MRI, are needed in order to verify these tendencies.

As one of the extrathalamic inputs, and the most extensive, cholinergic afferents center in the NBM from where they are distributed throughout the cerebral cortex [7,27]. According to these widespread projections, the cholinergic modulation of the NBM has been implicated to play an important role in distinct neurobehavioral functions, such as attention, arousal, memory, and food intake [13,15,28]. The tendency of lower  $V_T$  in this region in the volunteers with obesity may hint to an altered cholinergic signaling, leading to increased food intake [29].

Paolone et al. [30] indicated impaired cholinergic stimulation of cortical circuitry through  $\alpha 4\beta 2^*$  nAChRs that were prone to attribute high-incentive salience to reward cues and poor attentional control as a vulnerability factor for obesity. Interestingly,  $\alpha 4\beta 2^*$  nAChR availability of the NBM was less correlated with those of all of the other brain regions, particularly in the normal-weight volunteers, while, in general,  $\alpha 4\beta 2^*$  nAChR availability appears to be more related to each other, probably indicating higher cholinergic tone in the volunteers with obesity.

The pathophysiological meaning of the putative differences in the  $\alpha 4\beta 2^*$  nAChRs is less clear. This could represent receptor desensitization, i.e., a loss of response after prolonged or repeated application of a stimulus [31], similar to tobacco use. In addition, constant stimulation of nAChRs in nicotine addiction can lead to receptor desensitization [32–34]. A tendency for lower nAChR availability in the volunteers with obesity could suggest a nAChR desensitization as an expression of a dysfunctional NBM.

In contrast, Buisson and Betrand [34] saw “hyperfunctional”  $\alpha 4\beta 2^*$  nAChRs after nicotine removal, even with an overall higher apparent affinity for ACh and currents of higher amplitudes with less desensitization. It seems that activation, as well as desensitization, contribute to the rewarding properties of nicotine inside of the cholinergic system [32].

With regard to the clinical implications, our investigation of  $\alpha 4\beta 2^*$  nAChRs goes beyond the current targets, such as dopamine and serotonin, and gives a perspective as a future molecular target for treating human obesity.

## 5. Limitations

These first data did not detect significant changes in  $\alpha 4\beta 2^*$  nAChR availability in obesity. This could be due to the relatively low number of participants included in the study. By applying the  $V_T$  results in the right NBM (difference of means 1.8, standard deviation 2.2) that were obtained in this study, we estimated a necessary sample size of 24 participants in each group for an independent *t*-test (alpha = 0.05, power = 0.8; power and sample size calculations; PS version 3.1.2; [35]) for future cross-sectional studies. Furthermore, we cannot estimate the time scales of the changes in  $\alpha 4\beta 2^*$  nAChR availability given the nature of these fast acting, allosteric receptors; rapid, dynamic interactions may also interfere at the individual signal level.

## 6. Conclusions

This is the first study on  $\alpha 4\beta 2^*$  nAChR that has used PET imaging in vivo and the high-affinity selective radiotracer (–)-[<sup>18</sup>F]flubatine to study human obesity. Overall, these first data showed no statistically significant  $V_T$  differences between the individuals with obesity and the normal-weight controls. However, these data also revealed trends toward lower  $\alpha 4\beta 2^*$  nAChR availability in the nucleus basalis of Meynert and higher  $\alpha 4\beta 2^*$  nAChR availability in the thalamus. Whether these tendencies become relevant in modulating eating behavior needs to be further explored, including studies that explore  $\alpha 4\beta 2^*$  nAChR availability with stimulation designs in order to define  $\alpha 4\beta 2^*$  nAChR as a promising target for future intervention.

**Author Contributions:** Conceptualization, M.R., P.M.M., G.-A.B., A.H., M.B., O.S. and S.H.; methodology, M.R., G.-A.B., M.P., A.H., O.S. and S.H.; validation, E.S.d.P., T.G., M.R., J.L., G.-A.B., S.M., A.H., O.S. and S.H.; formal analysis, E.S.d.P., T.G., M.R., J.L., G.-A.B., O.S. and S.H.; investigation, E.S.d.P., T.G., M.R., J.L., P.M.M., S.M. and S.H.; resources, M.P., A.H., M.B. and O.S.; software, M.R. and G.-A.B.; data curation, E.S.d.P., T.G., M.R., J.L., G.-A.B., P.M.M., S.M. and S.H.; writing—original draft preparation, E.S.d.P., T.G., M.R., J.L., G.-A.B. and S.H.; writing—review and editing, M.K.H., P.M.M., M.P., S.M., A.H., M.B., O.S. and S.H.; visualization, E.S.d.P., J.L. and M.R.; supervision, O.S. and S.H.; project administration, O.S. and S.H.; funding acquisition, A.H., M.B., O.S. and S.H. All authors have read and agreed to the published version of the manuscript.

**Funding:** This work was supported by the IFB Adiposity Diseases, Federal Ministry of Education and Research (BMBF), Germany; FKZ 01E01501 (<http://www.bmbf.de>, accessed on 1 October 2022).

**Institutional Review Board Statement:** The study was performed according to the 1964 declaration of Helsinki and subsequent revisions and was approved by the local ethics committee (number 225-15-01062015; date of approval 18th of June 2015), as well as the national radiation protection agency.

**Informed Consent Statement:** Written informed consent was obtained from all of the participants included in the study.

**Data Availability Statement:** The data presented in this study are available upon request from the corresponding author. The data are not publicly available due to the fact that they contain information that could compromise the privacy of the participants.

**Acknowledgments:** These data were part of the presentation at the 11th European Conference on Clinical Neuroimaging (ECCN, 14–15 March 2022), Geneva, Switzerland.

**Conflicts of Interest:** The authors declare no conflict of interest.

## References

- Bessesen, D.H. Update on Obesity. *J. Clin. Endocrinol. Metab.* **2008**, *93*, 2027–2034. [[CrossRef](#)]
- Stojakovic, A.; Espinosa, E.P.; Farhad, O.T.; Lutfy, K. Effects of nicotine on homeostatic and hedonic components of food intake. *J. Endocrinol.* **2017**, *235*, R13–R31. [[CrossRef](#)]
- Zoli, M.; Picciotto, M. Nicotinic Regulation of Energy Homeostasis. *Nicotine Tob. Res.* **2012**, *14*, 1270–1290. [[CrossRef](#)] [[PubMed](#)]
- Fallon, S.; Shearman, E.; Sershen, H.; Lajtha, A. Food Reward-Induced Neurotransmitter Changes in Cognitive Brain Regions. *Neurochem. Res.* **2007**, *32*, 1772–1782. [[CrossRef](#)] [[PubMed](#)]
- Janssen, L.K.; Horstmann, A. Molecular Imaging of Central Dopamine in Obesity: A Qualitative Review across Substrates and Radiotracers. *Brain Sci.* **2022**, *12*, 486. [[CrossRef](#)]
- Collins, A.L.; Aitken, T.J.; Greenfield, V.Y.; Ostlund, S.B.; Wassum, K.M. Nucleus Accumbens Acetylcholine Receptors Modulate Dopamine and Motivation. *Neuropsychopharmacology* **2016**, *41*, 2830–2838. [[CrossRef](#)] [[PubMed](#)]
- Dani, J.A.; Bertrand, D. Nicotinic Acetylcholine Receptors and Nicotinic Cholinergic Mechanisms of the Central Nervous System. *Annu. Rev. Pharmacol. Toxicol.* **2007**, *47*, 699–729. [[CrossRef](#)]
- Picard, F.; Sadaghiani, S.; Leroy, C.; Courvoisier, D.S.; Maroy, R.; Bottlaender, M. High density of nicotinic receptors in the cingulo-insular network. *NeuroImage* **2013**, *79*, 42–51. [[CrossRef](#)]
- Sabri, O.; Becker, G.-A.; Meyer, P.M.; Hesse, S.; Wilke, S.; Graef, S.; Patt, M.; Luthardt, J.; Wagenknecht, G.; Hoeppe, A.; et al. First-in-human PET quantification study of cerebral  $\alpha 4\beta 2^*$  nicotinic acetylcholine receptors using the novel specific radioligand (–)-[<sup>18</sup>F]Flubatine. *NeuroImage* **2015**, *118*, 199–208. [[CrossRef](#)]
- Pistelli, F.; Aquilini, F.; Carrozzi, L. Weight gain after smoking cessation. *Monaldi Arch. Chest Dis.* **2009**, *71*, 81–87. [[CrossRef](#)]
- Kovacs, M.A.; Correa, J.B.; Brandon, T.H. Smoking as alternative to eating among restrained eaters: Effect of food prime on young adult female smokers. *Heal. Psychol.* **2014**, *33*, 1174–1184. [[CrossRef](#)] [[PubMed](#)]
- Pilhatsch, M.; Scheuing, H.; Kroemer, N.; Kobiella, A.; Bidlingmaier, M.; Farger, G.; Smolka, M.N.; Zimmermann, U.S. Nicotine administration in healthy non-smokers reduces appetite but does not alter plasma ghrelin. *Hum. Psychopharmacol. Clin. Exp.* **2014**, *29*, 384–387. [[CrossRef](#)] [[PubMed](#)]
- Mineur, Y.S.; Abizaid, A.; Rao, Y.; Salas, R.; DiLeone, R.J.; Gündisch, D.; Diano, S.; De Biasi, M.; Horvath, T.L.; Gao, X.-B.; et al. Nicotine Decreases Food Intake Through Activation of POMC Neurons. *Science* **2011**, *332*, 1330–1332. [[CrossRef](#)]
- Huang, H.; Xu, Y.; van den Pol, A.N. Nicotine excites hypothalamic arcuate anorexigenic proopiomelanocortin neurons and orexigenic neuropeptide Y neurons: Similarities and differences. *J. Neurophysiol.* **2011**, *106*, 1191–1202. [[CrossRef](#)] [[PubMed](#)]
- Picciotto, M.R.; Kenny, P.J. Molecular Mechanisms Underlying Behaviors Related to Nicotine Addiction. *Cold Spring Harb. Perspect. Med.* **2012**, *3*, a012112. [[CrossRef](#)]
- Ferreira, M.; Sahibzada, N.; Shi, M.; Panico, W.; Niedringhaus, M.; Wasserman, A.; Kellar, K.J.; Verbalis, J.; Gillis, R.A. CNS Site of Action and Brainstem Circuitry Responsible for the Intravenous Effects of Nicotine on Gastric Tone. *J. Neurosci.* **2002**, *22*, 2764–2779. [[CrossRef](#)] [[PubMed](#)]

17. Seeley, R.J.; Sandoval, D.A. Neuroscience: Weight loss through smoking. *Nature* **2011**, *475*, 176–177. [[CrossRef](#)] [[PubMed](#)]
18. Hillmer, A.; Esterlis, I.; Gallezot, J.; Bois, F.; Zheng, M.; Nabulsi, N.; Lin, S.; Papke, R.; Huang, Y.; Sabri, O.; et al. Imaging of cerebral  $\alpha 4\beta 2^*$  nicotinic acetylcholine receptors with  $(-)-[^{18}\text{F}]\text{Flubatine}$  PET: Implementation of bolus plus constant infusion and sensitivity to acetylcholine in human brain. *NeuroImage* **2016**, *141*, 71–80. [[CrossRef](#)]
19. Stunkard, A.J.; Messick, S. The three-factor eating questionnaire to measure dietary restraint, disinhibition and hunger. *J. Psychosom. Res.* **1985**, *29*, 71–83. [[CrossRef](#)]
20. Patt, M.; Schildan, A.; Habermann, B.; Fischer, S.; Hiller, A.; Deuther-Conrad, W.; Wilke, S.; Smits, R.; Hoepping, A.; Wagenknecht, G.; et al. Fully automated radiosynthesis of both enantiomers of  $[^{18}\text{F}]\text{Flubatine}$  under GMP conditions for human application. *Appl. Radiat. Isot.* **2013**, *80*, 7–11. [[CrossRef](#)]
21. Catana, C.; van der Kouwe, A.; Benner, T.; Michel, C.J.; Hamm, M.; Fenchel, M.; Fischl, B.; Rosen, B.; Schmand, M.; Sorensen, A.G. Toward Implementing an MRI-Based PET Attenuation-Correction Method for Neurologic Studies on the MR-PET Brain Prototype. *J. Nucl. Med.* **2010**, *51*, 1431–1438. [[CrossRef](#)] [[PubMed](#)]
22. Gielow, M.R.; Zaborszky, L. The Input-Output Relationship of the Cholinergic Basal Forebrain. *Cell Rep.* **2017**, *18*, 1817–1830. [[CrossRef](#)] [[PubMed](#)]
23. Ding, J.B.; Guzman, J.N.; Peterson, J.D.; Goldberg, J.A.; Surmeier, D.J. Thalamic Gating of Corticostriatal Signaling by Cholinergic Interneurons. *Neuron* **2010**, *67*, 294–307. [[CrossRef](#)] [[PubMed](#)]
24. Halassa, M.M.; Kastner, S. Thalamic functions in distributed cognitive control. *Nat. Neurosci.* **2017**, *20*, 1669–1679. [[CrossRef](#)] [[PubMed](#)]
25. Schmitt, L.I.; Wimmer, R.D.; Nakajima, M.; Happ, M.; Mofakham, S.; Halassa, M.M. Thalamic amplification of cortical connectivity sustains attentional control. *Nature* **2017**, *545*, 219–223. [[CrossRef](#)] [[PubMed](#)]
26. Hesse, S.; Rullmann, M.; Becker, G.A. Simultaneous assessment of  $\alpha 4\beta 2$  nicotinic acetylcholine receptor (nAChR) availability and neuronal response to rewarding food-cues in human obesity using PET-MRI. *J. Cereb. Blood Flow Metab.* **2021**, *41* (Suppl. 1), 233–234. [[CrossRef](#)]
27. Mesulam, M.-M. Cholinergic circuitry of the human nucleus basalis and its fate in Alzheimer’s disease. *J. Comp. Neurol.* **2013**, *521*, 4124–4144. [[CrossRef](#)]
28. Croxson, P.; Kyriazis, D.A.; Baxter, M.G. Cholinergic modulation of a specific memory function of prefrontal cortex. *Nat. Neurosci.* **2011**, *14*, 1510–1512. [[CrossRef](#)]
29. Herman, A.M.; Ortiz-Guzman, J.; Kochukov, M.; Herman, I.; Quast, K.B.; Patel, J.M.; Tepe, B.; Carlson, J.C.; Ung, K.; Selever, J.; et al. A cholinergic basal forebrain feeding circuit modulates appetite suppression. *Nature* **2016**, *538*, 253–256. [[CrossRef](#)]
30. Paolone, G.; Angelakos, C.C.; Meyer, P.J.; Robinson, T.E.; Sarter, M. Cholinergic Control over Attention in Rats Prone to Attribute Incentive Salience to Reward Cues. *J. Neurosci.* **2013**, *33*, 8321–8335. [[CrossRef](#)]
31. Ochoa, E.L.M.; Chattopadhyay, A.; McNamee, M.G. Desensitization of the nicotinic acetylcholine receptor: Molecular mechanisms and effect of modulators. *Cell. Mol. Neurobiol.* **1989**, *9*, 141–178. [[CrossRef](#)] [[PubMed](#)]
32. Picciotto, M.R.; Addy, N.A.; Mineur, Y.S.; Brunzell, D.H. It is not “either/or”: Activation and desensitization of nicotinic acetylcholine receptors both contribute to behaviors related to nicotine addiction and mood. *Prog. Neurobiol.* **2008**, *84*, 329–342. [[CrossRef](#)] [[PubMed](#)]
33. Bentley, P.; Driver, J.; Dolan, R. Cholinergic modulation of cognition: Insights from human pharmacological functional neuroimaging. *Prog. Neurobiol.* **2011**, *94*, 360–388. [[CrossRef](#)] [[PubMed](#)]
34. Buisson, B.; Bertrand, D. Chronic Exposure to Nicotine Upregulates the Human  $\alpha 4\beta 2$  Nicotinic Acetylcholine Receptor Function. *J. Neurosci.* **2001**, *21*, 1819–1829. [[CrossRef](#)] [[PubMed](#)]
35. Dupont, W.D.; Plummer, W.D. Power and sample size calculations: A review and computer program. *Control. Clin. Trials* **1990**, *11*, 116–128. [[CrossRef](#)]